Auto Disturbance Rejection Speed Control of Linear Switched Reluctance motor

J.F. Pan, IEEE Student Member, Kwok San Chin and N.C. Cheung, IEEE Member,
Dept. of Electrical Engineering,
Hong Kong Polytechnic University, Hong Kong
eencheun@inet.polyu.edu.hk

Jinming Yang,
Dept. of Electrical Engineering,
Electrical Power College, South China University of Technology, Guangzhou, China
jmyang@scut.com.cn

Abstract— **This paper describes the control of a Linear Switched Reluctance Motor (LSRM) using the Auto Disturbance Rejection Speed Controller (ADRC). The LSRM has the advantages of low cost, simple construction, and high reliability. However, being a direct-drive system, it is susceptible to parameter variations and load disturbances. ADRC controller has the natural ability to adapt to parameter variations; therefore it is a good candidate for the control of LSRM. In this paper, both the simulation and the hardware implementation of the ADRC on LSRM have been carried out. Results show that the controller has robust and reliable features. It can withstand large parameter variations and load disturbances, and it is much superior to cascade type PID controllers.**

Keywords-Direct-drive system; LSRM; ADRC;

I. INTRODUCTION

With the continual development of power electronics and advanced control strategies, there is an increasing interest in direct-drive machines, which directly convert electrical energy into kinetic motion without the support of mechanical translators. This type of machine can avoid backlash or hysteresis, thereby reducing the need for frequent mechanical adjustments or maintenance. Overall, direct-drive motors have the advantages of simple control, fast response, high speed, and high acceleration.

A linear switched reluctance motor (LSRM) is an example of such type of machine. Compared with other types of linear motor, such as linear permanent magnetic motor (LPMM) or linear induction motor (LIM), LSRM has advantages of simple structure, high robustness, and no expensive magnets. The whole motor contains only laminated steel plates and coil windings. Such a motor has been reported by the author in the past [1]. In this paper, an improved version of the LSRM, together with the implementation of a novel control strategy, are reported.

The LSRM consists of a moving platform, a pair of linear motion guides, laminated plates located at the base. The moving platform plate and the stands are made of aluminum to minimize the moving mass and to facilitate the magnetic path. The laminated plate is made of 0.5mm thick silicon-steel plate. The plates are grouped together for every 50 pieces.

The mover consists of three coils. The coils are winded onto the steel plates which are mounted on the mover by special stands. The coils are driven by 3 different separate currents, each with a 120 electrical degree separation. With such a configuration, the mutual inductance could be minimized [2]. The air gap between the upper moving plates and the lower fixed plates is kept at 0.2mm for optimal horizontal force output. The attraction force between magnetic circuits of the mover and the stator track is very strong; to provide a rigid structure, locking pins are inserted into the laminated plates of the mover, and clamping bars are mounted on the stator track to press down the stator laminated plates. Fig. 1 shows the construction of this motor.

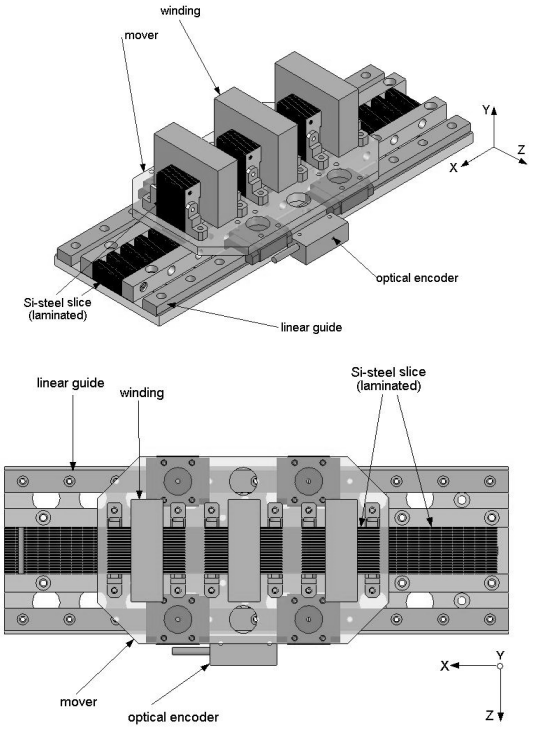

Fig.1 Perspective view of LSRM

Compared with the earlier developed machine in our laboratory [1], this actuator has a higher force output. Since the stator plates are held and pressed tightly in slots, the motor structure is more rigid, thus it is more resistant to mechanical

disturbances. It can avoid mechanical deformation of the air-gap when large values of current are injected into the windings.

TABLE I. SUMMARIZES THE MOTOR'S SPECIFICATIONS

Motor Parameters	
Pole width	6 mm
Pole pitch	12 mm
Motor length	135 mm
Phase separation	10 mm
Air gap width	0.2 mm
Number of turns per phase	160
Phase resistance	1.5 Ω

To ensure optimal speed regulation, this paper presents an auto-disturbance rejection controller (ADRC) for the control strategy implementation. This newly proposed control scheme [3] does not rely on detailed modeling of the motor, as in state-space control. Besides, the controller's robust feature outperforms classical PID controllers, because the unpredictable variables can compose of model dynamics, internal uncertainties and external disturbances. Simulation and implementation results show that the motor behaves more robustly and has a better dynamic performance under disturbing environment.

II. THE AUTO DISTURBANCE REJECTION CONTROLLER (ADRC)

A typical ADRC is shown in Fig. 2. It consists of the following parts:

a. Tracking differentiator (TD)

b. Nonlinear state error feedback (NLSEF)

c. Extended state observer (ESO)

A tracking differentiator is responsible for the arrangement of an appropriate transient process and provides proper differential signals of each order; The NLSEF block determines control input by tracking error signal and its different formats (derivatives/integrals) for optimal combination with nonlinear algorithms for output;

The extended state observer is the essential part of an ADRC. It is capable of observing state variables of each order and the "extended state", which includes the combined unpredictable (model uncertainties and external disturbances), in real-time and fed them back for system compensation.

A. The Tracking Differentiator (TD)

In motor control systems, the differential signal is usually obtained by backward difference of the given signal such as position, which may contains certain amount of stochastic noise or it is difficult to pick out [4]. TD is applied to alleviate the problem of differential signals extraction [5]. A second-order TD takes in the reference signal as input and outputs two signals: transient arrangement of input signal and its first differential.

Generally TD takes the following form of,

$$\begin{cases} \varepsilon_0 = v_1 - v^* \\ \dot{v}_1 = -r * fal(\varepsilon_0, a_0, \delta_0) \end{cases} \quad (1)$$

where v* is reference velocity, v1 is its tracking signal, r, a0 and δ_0 are parameters to be regulated. The fal function is expressed as,

$$fal(\varepsilon, a, \delta) = \begin{cases} |\varepsilon|^a \operatorname{sgn}(\varepsilon), & |\varepsilon| > \delta \\ \dfrac{\varepsilon}{\delta^{1-a}}, & |\varepsilon| \le \delta \end{cases} \quad (2)$$

B. The Extended State Observer (ESO)

An extended state observer (ESO) is designed for a class of nonlinear system [6],

$$N(t) = f(x, \dot{x}, ..., x^{(n-1)}(t), t) + w(t) \quad (3)$$

where $f(x, \dot{x}, ..., x^{(n-1)}, t)$ represents an unknown function, w(t) the unknown disturbances. The goal is to build an observer to observe each state variable x , $\dot{x}$,..., and $x^{(n-1)}$ correctly in despite of detailed format of $f(x, \dot{x}, ..., x^{(n-1)}, t)$ and w(t).

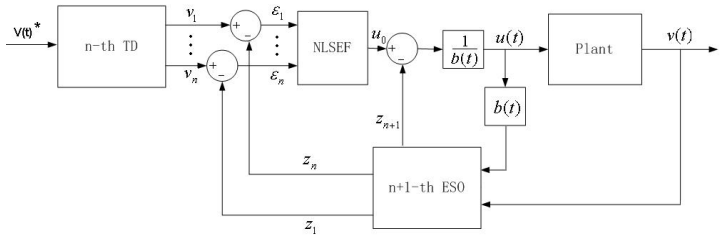

Fig2. Structure of an ADRC

For convenience, we include $x^{(n)}(t)$ as the extended state variable and construct the following system,

$$\begin{cases} \varepsilon = z_1 - x(t) \\ \dot{z}_1 = z_2 - g_1(\varepsilon) \\ \dot{z}_2 = z_3 - g_2(\varepsilon) \\ \vdots \\ \dot{z}_{n+1} = -g_{n+1}(\varepsilon) \end{cases} \tag{4}$$

There exist functions $g_1 \sim g_{n+1}$, so that the above differential equations satisfies,

$$z_1(t) \to x(t) \ldots\ldots z_{n+1}(t) \to x^{(n)}(t)$$

The above conclusion provides a common procedure for the construction for an ESO structure. We can leave all unknown factors of any kind as a whole part, and construct an object equation with the format (4). Analysis of the performance of a second-order ESO can be found in [7].

C. *The Nonlinear state error feedback (NLSEF)*

In a PID controller, error's past, present and future behaviors are treated simply by linear summations. In an ADRC, different error formats from the TD output are combined with nonlinear algorithm and the weighting factors of each error state can be regulated according to the actual system performance.

A typical nonlinear relationship for a n-th NLSEF can be expressed as [8],

$$u_0 = k_1 fal(\varepsilon_1, \alpha, \delta) + \ldots + k_n fal(\varepsilon_n, \alpha, \delta) \tag{5}$$

where ki (i=1, 2, …,k), α , and δ are parameters to regulated. ε_i is error signal and its derivatives are obtained from a n-th TD before the NLSEF block. The fal function is derived from equation (2).The reason why a nonlinear combination of error signals over a linear one is because there is a linear region when the error ε falls into the intervals of $\pm\delta$ while the gain diminishes accordingly when the error is getting larger. This avoids excessive gain when error is small, which might lead to high frequency chattering [9].

The controller for the system thus can be expressed as,

$$u(t) = (u_0(t) - a(t)) / b \tag{6}$$

where a(t) is the observation of total uncertainties and disturbances from ESO.

III. CONTRUNCTION OF THE ADRC CONTROLLER

For SR motors, the disturbances may include change of load/friction, mover mass variation or control signal fluctuation such as force or current ripples.

The force equation of the LSRM can be represented as,

$$M\dot{V} + BvV + f_l(t) = \sum_{k=a}^{c} f_k(i_k(t), x(t)) = u_q \tag{7}$$

Where uq is the totally generated electromechanical force, fl(t) is load force, and M, Bv are the mover mass and friction constant, respectively. If disturbances and uncertainties of mass, friction and force variations are concerned, then the equation becomes,

$$\dot{V} = (\triangle B + B_m)V + (\triangle A + A_m) f_l + (\triangle A + A_m) u_q \tag{8}$$

where $B_m = \frac{-B_v}{M}$, $A_m = \frac{-1}{M}$ and $\triangle B$, $\triangle A$ are parameter variations. The equation can be further represented as,

$$\begin{aligned} \dot{V} &= F_w + B_m V + A_m u_q \\ &= F_w - \frac{B_v}{M} V + \frac{1}{M} u_q \\ &= a(t) + b u_q \end{aligned} \tag{9}$$

where $F_w = \triangle BV + (\triangle A + A_m) f_l + \triangle A u_q$ which includes all external disturbances and system uncertainties; b = 1/M and a(t)= $F_w - \frac{B_v}{M} V$. The above differential equation for velocity only include a. the compositive uncertainties a(t) and b. the control parameter bu_q . Therefore, if the compositive item can be observed correctly by the ADRC and fed back to the system, the model of this SR motor becomes a first-order system.

The control object is focused on velocity. The input for TD is speed command and it will arrange a proper transient process which has the output of,

$$V1(t) = -r\_T \cdot fal(V1 - V, \delta\_T, \alpha\_T) \tag{10}$$

where r_T, δ_T and α_T are parameters to be regulated. Then the output V1 is compared with observed speed state fed back from ESO, and the difference is determined by NLSEF block to give a proper u0,

$$u_0 = \beta\_N \cdot fal(\varepsilon, \delta\_N, \alpha\_N) \tag{11}$$

Three more values β_N , δ_N and α_N for regulation are included. Then the control force input uq for the motor becomes,

$$u_q = \frac{1}{b}(u_0 - Z_2) \tag{12}$$

b is a constant value and b=1/M. The actual measured velocity value Vbak from the encoder will be fed back to ESO for state observation, the velocity state Z1 and the extended state Z2 are derived from the following,

$$\begin{cases} \dot{Z}_1 = bu_q + Z_2 - \beta_{01\_E} \cdot fal(Z_1 - V_{bak}, \delta_{EX}, \alpha_E) \\ \dot{Z}_2 = -\beta_{02\_E} \cdot fal(Z_1 - V_{bak}, \delta_E, \alpha_E) \end{cases} \tag{13}$$

Again, four parameters β_{01_E} , β_{02_E} , δ_E and α_E to be regulated are introduced.

Therefore the whole control block can be derived from the above and is shown in Fig. 3.

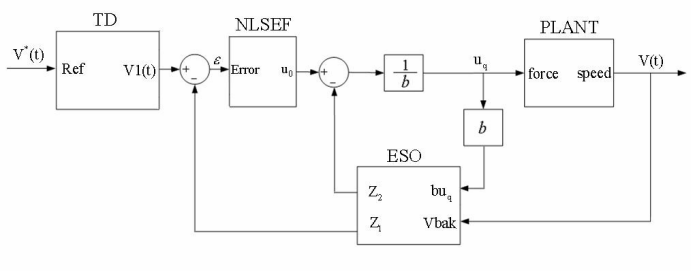

Fig.3 Control system block diagram

Concerning the parameter regulations of an ADRC, the whole system is adjusted empirically on simulation and experiment basis. The parameters for TD block are mainly based on the arrangement of a proper transient process and the capability of successfully tracking reference signal within certain error range [5]. ESO can be configured according to "pole-zero assignment" [6, 7] method above to observe every state of each order correctly and estimate the whole unpredictable (extended state) precisely. NLSEF decides the stable error and it can be designed on such a basis [8].

On the motor's side, first a region decision mechanism shall take the combined force command uq from the ADRC controller. Then according to the mover's current position, required force value for each phase is calculated. The amount of force value and corresponding phase(s) to be excited are acquired based on mover's current position and the direction the mover required to advance. If two phases are required to be simultaneously excited, a simple linear distribution rule is employed [11].

After the force command for each phase is obtained, the required current value shall be calculated. Instead of using the lookup table linearization scheme proposed in [11], we employ a simple relationship between force and current for linear region calculation [12]. This can reduce memory and calculation burden on the DSP. The force function of current and position is expressed as,

$$f(x,i) = \frac{\pi i^2 \Delta L}{P} \cdot \sin(\frac{2\pi x}{P}) \tag{14}$$

where P, x and i are pole pitch, travel distance and phase current respectively; $2\Delta L$ is the change of phase inductance from aligned to unaligned position. Therefore the reverse relationship of current with force and position can be easily calculated [11, 12].

IV. SIMULATION AND EXPERIMENTS RESULES

A. Simulation Result

To verify the proposed control scheme, simulations focused on the comparisons between an ADRC and a PID controller have been carried out. They are performed under the following conditions,

M=3M0

Load=20N

Force ripple increase about 20%

Friction increase 10%

Sudden change of the above parameters occurs at time=0.2s for all cases. The PID parameters are selected according to a typical dynamic response of the system; The parameters for the ADRC are selected according to the response of the system. They are further fine-tuned by repeated trial-and-error.

Fig. 5 shows that the PID controller has reasonable recover time; tracking is just satisfactory if the mass or friction does not change. The result is very dependent on mass and force variations. For the motor system under ADRC, the response remains the same for all the situations. The simulation results prove the ADRC has higher robustness.

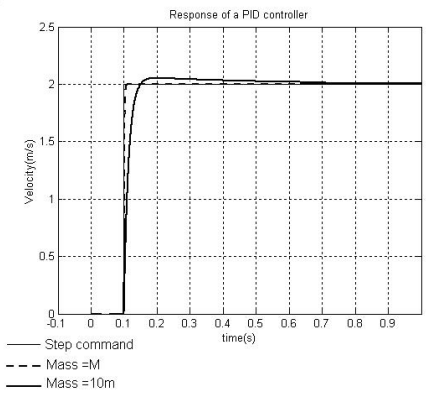

(a)

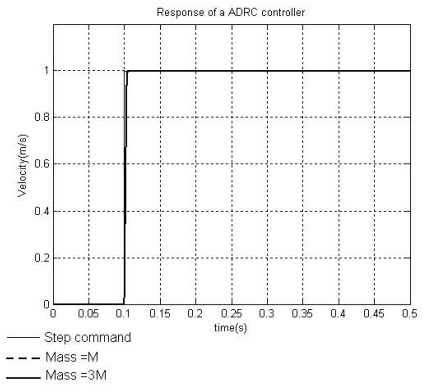

(b)

Fig.4 Responses of mass change (a) PID (b) ADRC

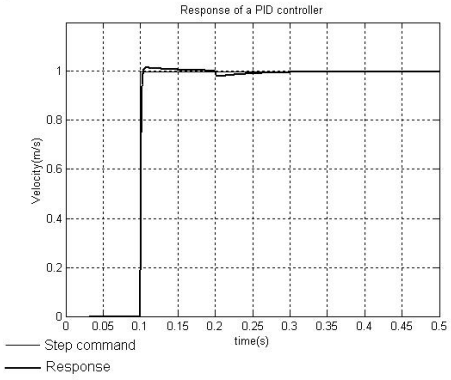

(a)

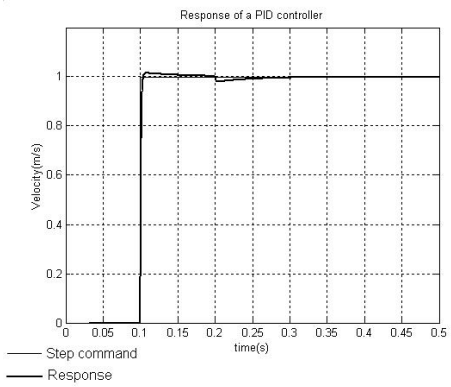

(b)

Fig.5 Response of PID with (a) load change and (b) friction change at 0.2s

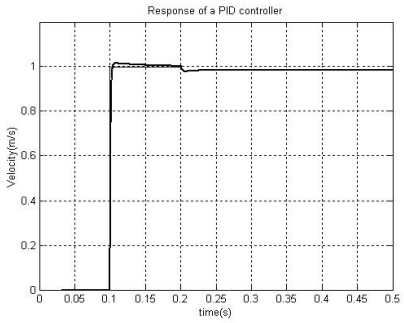

(a)

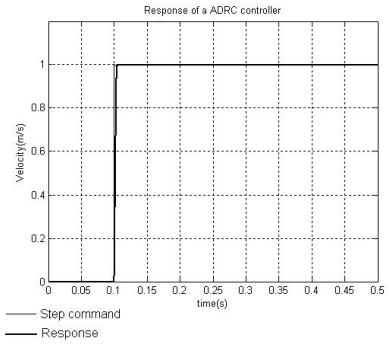

(b)

Fig. 6 Responses of PID and ADRC controller at force change at 0.2s

B. Experiment Results

The whole experiment is conducted on a dSPACE DS1104 controller card. The card interfaces with PC through the PCI bus. Position and velocity feedback signal is collected by an optical encoder fixed on the mover; Output current is generated by the controller card and passes to the motor driver through the Digital to Analogue Channel (DAC). Current feedback is obtained by the current transducers; it is then fed back to the dSPACE card through Analogue to Digital Channel (ADC). The whole experiment is operated in real-time and the sampling frequency is 10 kHz for the inner current loop and 2 kHz for

the outer velocity loop. Fig. 7 shows the whole experimental setup.

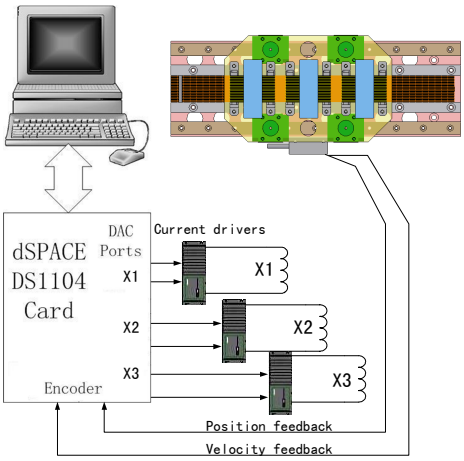

Fig.7 The experimental setup

The experiment is based on the behaviors of the motor with different controllers under disturbance environments. Before any disturbance is added, each controller has been regulated, as shown in table 2. Thereafter, the experiment with disturbances is tested with controller parameters remained unchanged.

Fig.8 (a) and (b) demonstrate the velocity & position response of PID and ADRC respectively when a steel block of mass 1kg is fixed on the mover. It can be seen that, for the PID controller, there are lots of noise when the motor is crossing the zero speed region. For the ADRC, the velocity profile is smooth, and the performance is independent of the mass change. This observation verifies the simulation result shown in Fig.4.

When a controlled force disturbance of about 2% is added to the two controllers, each encounters a sudden change accordingly. The noise from the PID becomes larger while the velocity tracking error recovers back to zero quickly, as shown in Fig. 9.

Friction is added to the motor with the help of a pull-spring, which has an elasticity coefficient of 35N/m. The motor is only under the pull of the spring in one direction of motion, but the force is varied at each position of the mover according to the stator. The velocity response profile in Fig. 10 shows that the speed variations are unbalanced for each direction of moving and the tracking error is much bigger for the PID controller. Therefore the ADRC is more robust.

TABLE II. ADRC PARAMETER REGULATIONS

PID			**ADRC**									
			TD			ESO				NLSEF		
P	D	I	r_T	a_T	δ_T	B01_E	B02_E	a_E	δ_E	B1_N	a_N	δ_N
4	0.5	0.1	100	0.9	0.1	1000	5	0.9	0.001	2	0.5	0.001

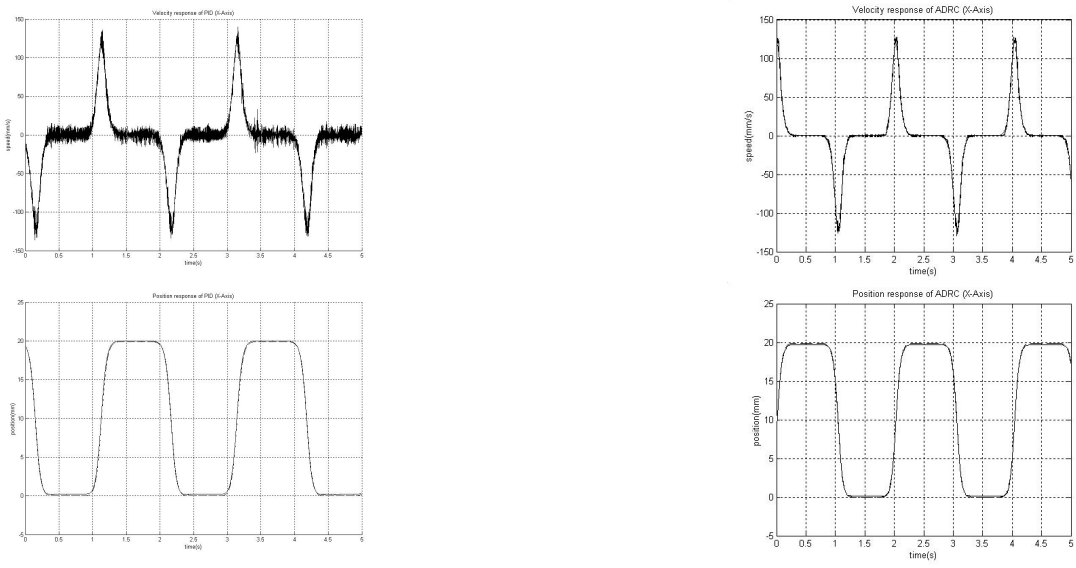

(a) (b)

Fig.8 Mass change of (a) PID and (b) ADRC response

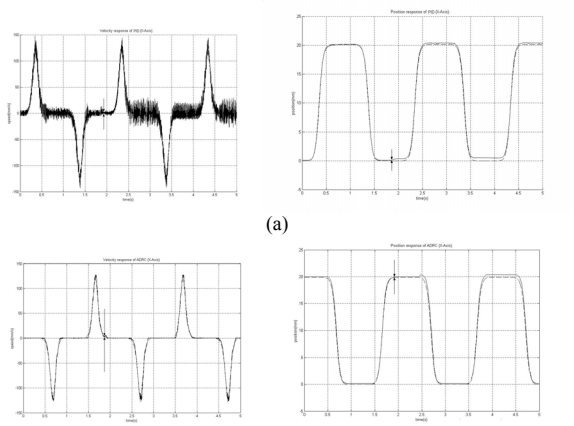

(a)

(b)

Fig. 9 Force command change of PID and ADRC response (a) PID and (b) ADRC response

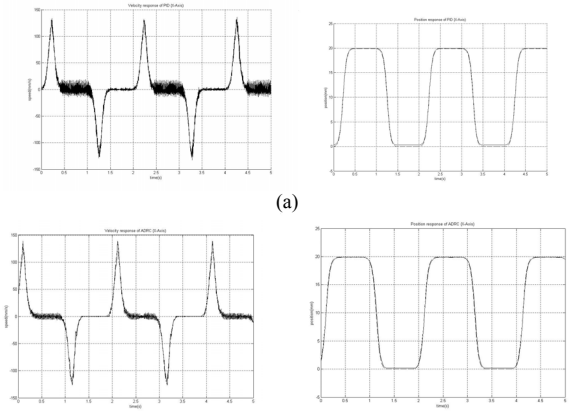

(a)

(b)

Fig. 10 Friction change response of PID and ADRC (a) PID and (b) ADRC response.

V. CONCLUSION

This paper proposes a novel, model-independent control scheme based on the Auto-Disturbance Rejection Controller (ADRC). With the implementation of this control strategy on the improved linear switched reluctance motor (LSRM), velocity control has been carried out. Performance comparisons are made with a classical PID controller. Simulation and experiment results demonstrate the motor is more resistant to disturbances under different operations. Therefore, the ADRC controller is very suitable for LSRM, especially when there is load disturbance and parameter variations.

ACKNOWLEDGEMENT

The authors would like to thank the Hong Kong Research Grants Council for the sponsoring of this research project under the project code B-Q473.

REFERENCE

[1] W. C. Gan and N. C. Cheung, "Design of a linear switched reluctance motor for high precision applications," in Proc. 3rd IEEE Int. Electric Machines and Drives Conf., June 2001, pp. 701–704.

[2] C. T. Liu and J. L. Kuo, "Experimental investigation and 3-D modeling of linear variable reluctance machine with magnetic-flux decoupled windings," IEEE Trans. Magn., vol. 30, pp. 4737–4739, Nov. 1994.

[3] Han Jingqing, "Auto-disturbances-rejection Controller and It's Applications", Trans. Control and Decision, China, vo1.13, no. 1, pp19-23, 1998. (In Chinese).

[4] Li Xu and Bin Yao, "Output feedback adaptive robust control of uncertain linear systems with large disturbances", American Control Conference, 1999. Proceedings of the 1999, Volume: 1, 2-4 June 1999, Pages: 556 - 560 vol.1.

[5] J.-Q. Han and W.Wang, "Nonlinear tracking differentiator," J. Syst. Sci.Math. Sci., vol. 14, no. 2, pp. 177−183, 1994. (In Chinese).

[6] Han Jingqing, "The Extended State Observer of a class of Uncertain Systems", Trans. on Control and Decision, China, vo1.10, no. 1, pp19-23, Jan, 1995. (In Chinese).

[7] Y. Huangand J. Han, "Analysis and design for the second order nonlinear continuous extended states observer," Chinese Sci. Bull., vol. 45, no. 21, pp. 1938−1944, 2000. (In Chinese).

[8] Han Jingqing, "Nonlinear state error feedback control law−NLSEF," Control and Decision, vol. 10, no. 3, pp. 221−225, 1995. (In Chinese).

[9] Zhiqiang Gao, Yi Huang, and Jingqing Han, "An alternative paradigm for control system design", Decision and Control, 2001. Proceedings of the 40th IEEE Conference, Volume: 5, 4-7 Dec. 2001, Pages: 4578 - 4585 vol.5

[10] Jianbo Su, Wenbin, etc. "Calibration-free robotic eye-hand coordination based on an auto disturbance-rejection controller", IEEE Transactions on Robotics, Volume: 20, Issue: 5, Oct.2004, Pages: 899 – 907.

[11] J.F. Pan, N.C. Cheung, and J.M. Yang, "High-Precision Position Control of a Novel Planar Switched Reluctance Motor", IEEE Transaction on Industrial Electronics. (To be published).

[12] I. Boldea and S. A. Nasar, *Linear Electric Actuator and Generator*, Cambridge University Press, 1997.

[13] Wai-Chuen Gan, Norbert C. Cheung, and Li Qiu, "Position Control of Linear Switched Reluctance Motors for High-Precision Applications", IEEE Trans. On Industry Applications, Vol. 39, No. 5, 2003, Pages: 1350–1362.